Hepatology Research

Hepatology Research 2014; 44: 1339–1346 doi: 10.1111/hepr.12309

Original Article

Hepatocellular carcinoma risk assessment using gadoxetic acid-enhanced hepatocyte phase magnetic resonance imaging

Nobutoshi Komatsu,[1] Utaroh Motosugi,[2] Shinya Maekawa,[1] Kuniaki Shindo,[1] Minoru Sakamoto,[1] Mitsuaki Sato,[1] Akihisa Tatsumi,[1] Mika Miura,[1] Fumitake Amemiya,[1] Yasuhiro Nakayama,[1] Taisuke Inoue,[1] Mitsuharu Fukasawa,[1] Tomoyoshi Uetake,[1] Masahiko Ohtaka,[1] Tadashi Sato,[1] Yasuhiro Asahina,[3] Masayuki Kurosaki,[4] Namiki Izumi,[4] Tomoaki Ichikawa,[2] Tsutomu Araki[2] and Nobuyuki Enomoto[1]

[1]*First Department of Internal Medicine,* [2]*Department of Radiology, University of Yamanashi, Yamanashi,* [3]*Department of Gastroenterology and Hepatology, Tokyo Medical and Dental University, and* [4]*Department of Gastroenterology and Hepatology, Musashino Red Cross Hospital, Tokyo, Japan*

Aim: To investigate whether the patients with hypovascular liver nodules determined on the arterial phase and hypointensity on the hepatocyte phase gadoxetic acid-enhanced magnetic resonance imaging (hypovascular hypointense nodules) are at increased risk of hepatocarcinogenesis, we assessed subsequent typical hepatocellular carcinoma (HCC) development at any sites of the liver with and without such nodules.

Methods: One hundred and twenty-seven patients with chronic hepatitis B or C and without a history of HCC, including 68 with liver cirrhosis, were divided into those with (non-clean liver group, $n = 18$) and without (clean liver group, $n = 109$) hypovascular hypointense nodules. All the patients were followed up for 3 years, and HCC development rates and risk factors were analyzed with the Kaplan–Meier method and the Cox proportional hazard model, respectively.

Results: A total of 17 patients (10 in the non-clean liver group and seven in the clean liver group) developed typical HCC. Cumulative 3-year rates of HCC development were 55.5% in the non-clean liver group and 6.4% in the clean liver group ($P < 0.001$), and those at the different sites from the initial nodules was also higher in the non-clean liver group (22.2%) than the clean liver group (6.4%) ($P = 0.003$). Multivariate analysis identified older age ($P = 0.024$), low platelet counts ($P = 0.017$) and a non-clean liver ($P < 0.001$) as independent risk factors for subsequent HCC development.

Conclusion: Patients with hypovascular hypointense liver nodules are at a higher risk for HCC development at any sites of the liver than those without such nodules.

Key words: gadoxetic acid, hepatocellular carcinoma, hepatocyte phase, magnetic resonance imaging, risk assessment

INTRODUCTION

HEPATOCELLULAR CARCINOMA (HCC) is one of the most common cancers worldwide and is a major cause of death in patients with chronic viral liver disease. Despite many advances in multidisciplinary treatment, complete curative treatment of early stage HCC remains the only possible therapeutic choice for long-term survival. Therefore, surveillance programs for patients at a high risk for HCC that include imaging-based evaluations are crucial for the detection and treatment of early stage HCC.

The newly introduced magnetic resonance imaging (MRI) contrast agent, gadolinium ethoxybenzyl

Correspondence: Dr Nobuyuki Enomoto, First Department of Internal Medicine, University of Yamanashi, 1110 Shimokato, Chuo, Yamanashi 409-3898, Japan. Email: enomoto@yamanashi.ac.jp

Conflict of interest: All authors have no conflict of interest related to this manuscript.

Funding: This study was supported in part by a Grant-in-Aid from the Ministry of Education, Science, Sports and Culture of Japan (23390195, 23791404, 24590964 and 24590965), and in part by a Grant-in-Aid from the Ministry of Health, Labor and Welfare of Japan (H23-kanen-001, H23-kanen-004, H23-kanen-006, H24-kanen-002, H24-kanen-004 and H25-kanen-006).

Received 18 August 2013; revision 13 January 2014; accepted 28 January 2014.

diethylenetriamine pentaacetic acid (gadoxetic acid), has enabled concurrent assessment of tumor vascularity and unique hepatocyte-specific contrast (hepatocyte phase).[1–3] This has led to the frequent identification of hypovascular nodules determined on the arterial phase with hypointensity on the hepatocyte phase (hypovascular hypointense nodules),[4–8] while many of these nodules are difficult to be detected by ultrasonography (US) or computed tomography (CT). Recently, the natural history of hypovascular hypointense nodules themselves were reported in several studies,[9–12] revealing the high risk of subsequent progress to typical HCC from these nodules. However, it is not well known whether patients with such nodules have a higher risk of developing typical HCC at any sites of the liver, including at the different sites from initial nodules, compared to those without such nodules.

If patients with these nodules may have a high risk of developing typical HCC not only at the same sites but also at the different sites from initial nodules, a significant proportion of these nodules are precancerous lesions or early stage HCC as reported,[13–15] and more importantly, the liver with these nodules may reflect a higher potential for hepatocarcinogenesis or the presence of undetectable precursor lesions in other sites of the liver. Conversely, the absence of these nodules potentially identifies the patients at a low risk for subsequent typical HCC development at any sites. The purpose of this study was to assess the risk of subsequent typical HCC development at any sites of the liver with and without hypovascular hypointense nodules on gadoxetic acid-enhanced MRI.

METHODS

Ethical review

THE PROTOCOL OF this retrospective study was approved by the ethics committee of Yamanashi University Hospital, which waived the requirement for written informed consent because the study was a retrospective data analysis, with appropriate consideration given to patient risk, privacy, welfare and rights.

Patients

We recruited 559 consecutive outpatients with chronic hepatitis B virus (HBV) or hepatitis C virus (HCV) infection who underwent gadoxetic acid-enhanced MRI at Yamanashi University Hospital between January 2008 and December 2010. The exclusion criteria were as follows: (i) presence or history of typical HCC ($n = 420$), because intrahepatic metastasis does not always develop through the usual multistep hepatocarcinogenesis process, skipping the early pathological stage with hypovascularity to an advanced pathological stage even when the size is small;[16,17] (ii) Child–Pugh class C disease ($n = 9$), because the hepatocyte phase findings are not reliable in patients with this condition because of reduced gadoxetic acid uptake in the liver;[18] and (iii) patients who dropped out during the 3-year follow-up period ($n = 3$).

After excluding 432 patients, 127 patients were included in this retrospective cohort study. They were divided into groups with hypovascular nodules determined on the arterial phase and hypointensity on the hepatocyte phase (non-clean liver group; $n = 18$ patients) and without such nodules (clean liver group; $n = 109$ patients) as shown in Figure 1. In this study, we divided cases into two groups according to the presence or absence of these nodules at the baseline, even when such nodules were initially detected during the follow-up period; we assigned these patients to the clean liver group.

Follow up and diagnosis of HCC

All 127 patients were followed up at the liver disease outpatient clinic of our institution with blood tests, including those for tumor markers and diagnostic imaging modality (US, CT or MRI). The development of typical HCC that required treatment as proposed by the American Association for the Study of Liver Diseases (AASLD) guidelines[19] and that was diagnosed according to imaging criteria, showing arterial hypervascularity and venous phase washout, or based on histological examination of liver biopsies from hypovascular nodules that grew to more than 10 mm during follow up. Biopsies were obtained using a 21-G core needle. Two patients each had a liver nodule of more than 10 mm in diameter on initial MRI (12 mm and 13 mm), which were diagnosed on the basis of the biopsy as dysplastic nodules.

The end-point of this study was the development of typical HCC not only from the hypovascular hypointense nodules observed initially but also from other areas without these nodules ("de novo HCC"). Dynamic CT and/or MRI were also performed in cases with hepatic nodules detected by US, liver cirrhosis, a tendency of tumor marker elevation and difficult evaluation of the liver parenchyma by US. All 127 patients were followed up for 3 years after the initial gadoxetic acid-enhanced MRI examination. When imaging

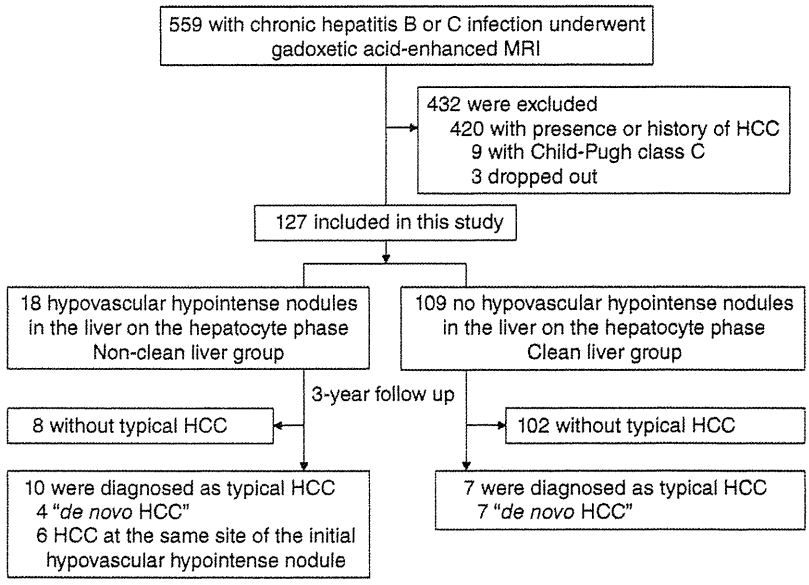

Figure 1 Patient inclusion criteria. "De novo HCC" is a typical hepatocellular carcinoma that developed at sites in which no nodules had been seen on the initial gadoxetic acid-enhanced magnetic resonance imaging (MRI).

modalities led to diagnosis of HCC, recognizing hypervascularization by more than one experienced radiologist and other imaging modalities was regarded as the time of diagnosis of HCC. When needle biopsy was performed to investigate nodules, the time of diagnosis of HCC was when the pathologists and physicians examined pathological tissue and diagnosed as HCC.

MRI

Magnetic resonance imaging was performed using a superconducting magnet that operated at 1.5 Tesla (Sigma EXCITE HD; GE Medical Systems, Milwaukee, WI, USA) and an 8-channel phased-array coil. First, we obtained fast spoiled gradient-echo T_1-weighted images (T1WI) with dual echo acquisition and respiratory-triggered fat-saturated fast spin-echo T_2-weighted images (T2WI). Dynamic fat-suppressed gradient-echo T1WI were obtained using a 3-D acquisition sequence before (precontrast) and 20–30 s, 60 s, 2 min, 5 min, 10 min and 20 min after the administration of gadoxetic acid (Primovist; Bayer Schering Pharma, Berlin, Germany). This contrast agent (0.025 mM/kg bodyweight) was administrated i.v. as a bolus at a rate of 1 mL/s through an i.v. cubital line (20–22 G) that was flushed with 20 mL saline from a power injector. The delay time for the arterial phase scan was adjusted according to a fluoroscopic triggering method.[20] All images were acquired in the transverse plane. Sagittal plane T1WI were also obtained during the hepatocyte phase at 20 min after the injection of the contrast agent.

Statistical analysis

All continuous values are expressed as median (range). Fisher's exact probability test was used for comparisons between categorical variable and the non-parametric Mann-Whitney *U*-test was used to compare differences between continuous variables. Baseline clinical characteristics, including blood test results, were evaluated within 1 month of the initial MRI. We investigated whether or not HCC development was associated with age, sex, fibrosis, etiology (HBV or HCV), platelet count, serum alanine aminotransferase (ALT), γ-glutamyltransferase (γ-GT), α-fetoprotein (AFP), and the presence or absence of hypovascular hypointense nodules.

Cumulative HCC development was estimated according to the Kaplan–Meier method and differences in the curves were tested using the log–rank test. Risk factors for HCC development were determined according to the Cox proportional hazard model. Subgroup analyses with a Cox proportional hazard model were applied to estimation of the hazard ratio (HR) of the non-clean liver group versus clean liver group in the dichotomized subgroups. All statistical analyses were performed using JMP software, version 10 (SAS Institute Japan, Tokyo, Japan). A two-sided *P*-value of less than 0.05 was considered statistically significant.

RESULTS

Characteristics of the patients and nodules

A TOTAL OF 127 patients were enrolled, of whom 26 had chronic HBV infections and 101 had HCV infections, and 68 had virus-associated cirrhosis. No statistically significant differences in the initial clinical characteristics were found between the non-clean liver and clean liver groups (Table 1). Thirty-five hypovascular hypointense nodules were found in 18 patients in the non-clean liver group (1–5 nodules per patient) at baseline (data not shown). Twenty-four of these 35 nodules were detectable only on the hepatocyte phase MRI and were undetectable by US, CT and non-hepatocyte phase MRI. None of the 35 nodules showed high intensity on T2WI. The median nodule diameter was 8 mm (range, 4–13 mm; 33 nodules with ≤10 mm, two nodules with 12 mm and 13 mm).

HCC incidence according to initial MRI findings

Hepatocellular carcinoma was diagnosed in 17 patients, 10 in the non-clean liver group and seven in the clean liver group; 14 of these patients had HCV infection. Thirteen patients were diagnosed according to the AASLD imaging criteria.[19] Four patients were diagnosed pathologically by liver biopsies that were performed, based on enlargement of the nodules of more than 10 mm in diameter during the observation period.

The cumulative 1-, 2- and 3-year HCC incidence rates were 1.5%, 10.2% and 13.4%, respectively. As determined by the Kaplan–Meier method, these rates were 11.1% (95% confidence interval [CI], 0.0–25.6%), 38.8% (95% CI, 16.3–61.4%) and 55.5% (95% CI, 32.6–78.5%) in the non-clean liver group, and 0.0% (95% CI, 0.0–2.3%), 5.5% (95% CI, 0.0–9.8%) and 6.4% (95% CI, 1.8–11.0%) in the clean liver group; the former group showed significantly higher rates of development of typical HCC than the latter ($P < 0.001$) as shown in Figure 2. The median imaging intervals were 3 months (range, 3–6) in the non-clean liver group and 4 months (range, 2–12) in the clean liver group. The imaging interval of the non-clean liver group was shorter than the clean liver group (3 vs 4 months, $P = 0.015$). The median intervals between the initial MRI and HCC diagnosis was 16 months (range, 9–32) in the non-clean liver group and 21 months (range, 16–35) in the clean liver group.

In 11 of 17 patients with HCC development, HCC developed at sites in which no nodules had been seen on the initial gadoxetic acid-enhanced MRI, namely de novo HCC. These HCC were found in four of 18 patients in the non-clean liver group (3-year HCC incidence rates: 22.2%; 95% CI, 4.3–51.0%) and 7 in 109 patients in the clean liver group (3-year HCC incidence rates: 6.4%; 95% CI, 1.8–11.0%). The incidence rates of de novo HCC was significantly higher in the non-clean liver group than the clean liver group ($P = 0.003$, Fig. 3). In the remaining six patients, HCC developed at the same site of the initial nodules exclusively in 18 patients of a non-clean liver group by definition, and those HCC arose among the nodules of 8 mm or more in the initial MRI study.

Risk factors for HCC development

Univariate analyses showed that the significant risk factors for HCC development included older age ($P = 0.039$), cirrhosis ($P = 0.009$), a low platelet count ($P = 0.003$), a high AFP concentration ($P = 0.006$) and a non-clean liver ($P < 0.001$). Multivariate analysis with these variables revealed that older age (hazard ratio [HR], 1.08; 95% CI, 1.01–1.16; $P = 0.024$), a low plate-

Table 1 Baseline patient characteristics

Characteristics	Total ($n = 127$)	Non-clean liver ($n = 18$)	Clean liver ($n = 109$)	P
Age, years	65 (30–88)	68 (46–82)	64 (30–88)	0.15
Male/female	68/59	10/8	58/51	1.00
Non-cirrhosis/cirrhosis	59/68	6/12	53/56	0.31
HBV/HCV	26/101	5/13	21/88	0.53
Platelet count ($\times 10^9$/L)	122 (30–410)	102 (46–187)	125 (30–410)	0.07
ALT (IU/L)	32 (7–206)	32 (14–95)	32 (7–206)	0.97
γ-GT (IU/L)	31 (9–305)	31 (13–258)	31 (9–305)	0.68
AFP (ng/mL)	4 (1–582)	8 (2–181)	4 (1–582)	0.19

Continuous data are shown as medians (range).
γ-GT, γ-glutamyltransferase; AFP, α-fetoprotein; ALT, alanine aminotransferase; HBV, hepatitis B virus; HCV, hepatitis C virus.

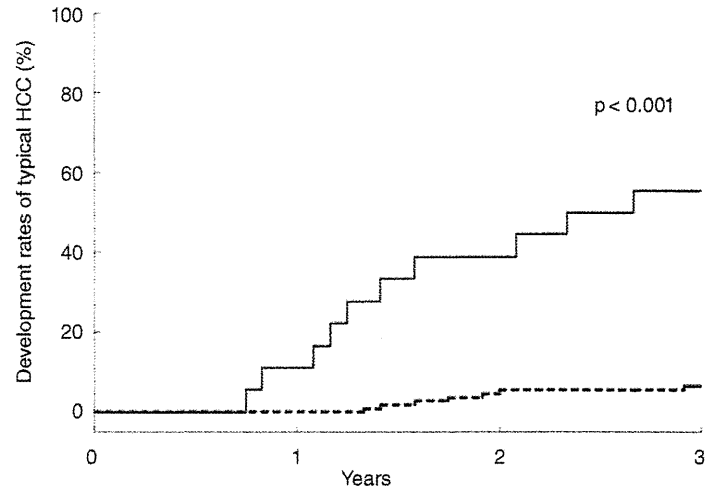

Figure 2 Cumulative incidence rates of typical hepatocellular carcinoma (HCC) development in the non-clean and clean liver groups. —, non-clean liver group ($n = 18$); ····, clean liver group ($n = 109$).

let count (HR, 1.17; 95% CI, 1.03–1.35; $P = 0.017$) and a non-clean liver (HR, 9.41; 95% CI, 3.47–25.46; $P < 0.001$) were the only independent risk factors for HCC development (Table 2).

We further assessed the effect of a non-clean liver on the risk of HCC development in subgroups of these patients (Fig. 4). We found that belonging to the non-clean liver group was a significant risk factor in patients without HBV. Notably, this designation was particularly valuable for patients who are generally regarded as at low risk for HCC development: those without cirrhosis (HR, 37.23; 95% CI, 3.30–419.71; $P = 0.003$) and those with high platelet counts (HR, 33.42; 95% CI, 6.69–166.94; $P < 0.001$).

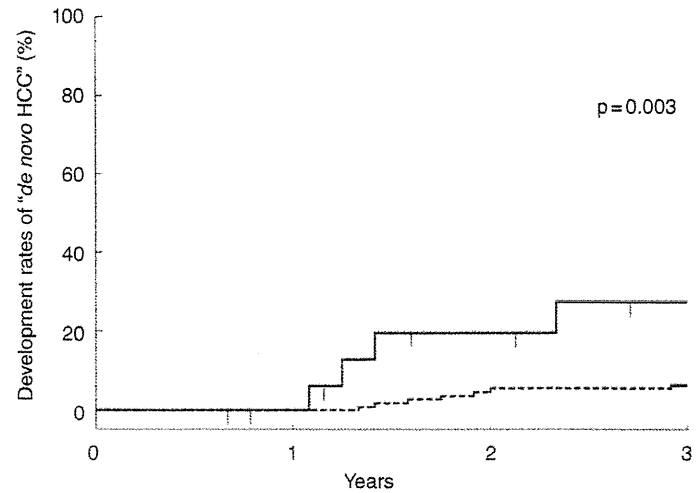

Figure 3 Cumulative incidence rates of typical hepatocellular carcinoma (HCC) at sites in which no nodules had been seen on the initial gadoxetic acid-enhanced magnetic resonance imaging, namely, "de novo HCC". —, non-clean liver group ($n = 18$); ····, clean liver group ($n = 109$).

Table 2 Variables that predict HCC development: univariate and multivariate analyses

Variables	Univariate		Multivariate	
	Hazard ratio (95% CI)	*P*	Hazard ratio (95% CI)	*P*
Male	0.56 (0.29–1.95)	0.755		
Age (per year)	1.06 (1.00–1.12)	0.039	1.08 (1.01–1.16)	0.024
Cirrhosis	14.37 (1.90–108.44)	0.009	3.54 (0.37–33.77)	0.231
HCV (vs HBV)	4.39 (0.58–33.17)	0.151		
Platelet count (per 10^{10}/L)	1.19 (1.06–1.33)	0.003	1.17 (1.03–1.35)	0.017
ALT (per IU/L)	1.00 (0.99–1.02)	0.423		
γ-GT (per IU/L)	1.00 (0.99–1.01)	0.688		
AFP >10 ng/mL	3.98 (1.47–10.77)	0.006	1.47 (0.49–4.33)	0.486
Non-clean liver	12.36 (4.68–32.61)	<0.001	9.41 (3.47–25.46)	<0.001

γ-GT, γ-glutamyltransferase; AFP, α-fetoprotein; ALT, alanine aminotransferase; CI, confidence interval; HBV, hepatitis B virus; HCC, hepatocellular carcinoma; HCV, hepatitis C virus.

DISCUSSION

THIS STUDY REVEALED presence of hypovascular hypointense liver nodules (non-clean liver) on gadoxetic acid-enhanced MRI, is a significant risk factor for subsequent development of typical HCC not only at the same sites but also at the different sites from the initial nodules. The incidence of development of typical HCC in the non-clean liver patients was more than 50% during a 3-year follow-up period, indicating that these higher risk patients should be rigorously investigated for the early detection of HCC during follow up.

In the present study, six of the 18 patients in the non-clean liver group developed typical HCC at the same site of the initial nodules during the subsequent 3 years (11.1%/year). Most of the hypovascular hypointense nodules on gadoxetic acid-enhanced MRI are considered precursor lesions of typical HCC, such as early HCC or high-grade dysplastic nodules, on histological examination,[13–15] while it has been reported that most hypovascular nodules exhibiting high-intensity to isointensity signals in the hepatocyte phase are benign hepatic nodules.[14,15] Recent studies have suggested that a reduction of organic anion-transporting polypeptide 1B3 (OATP 8) transporter expression begins at the earliest stage of hepatocarcinogenesis,[21,22] before changes in vascularity such as decreased portal flow or increased arterial flow. The progression rate of the small

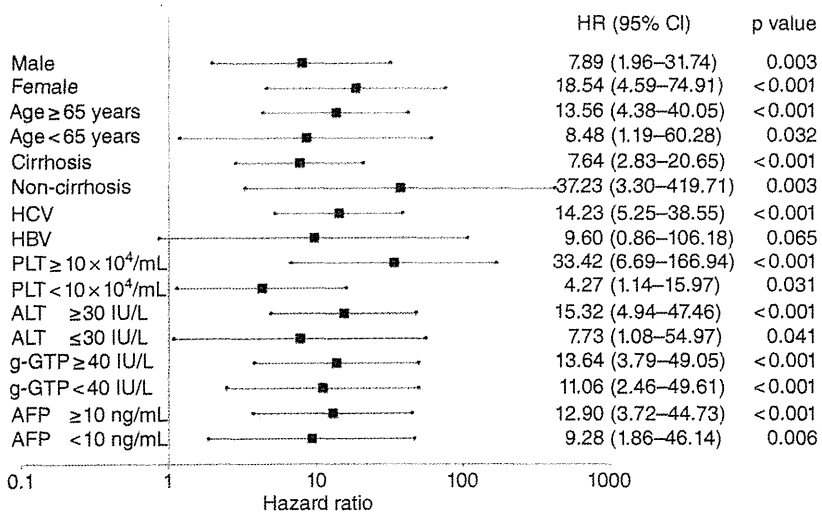

Figure 4 Stratified analyses of the non-clean liver as a risk factor for typical HCC development. AFP, α-fetoprotein; ALT, alanine aminotransferase; CI, confidence interval; g-GTP, γ-glutamyltransferase; HBV, hepatitis B virus; HCC, hepatocellular carcinoma; HCV, hepatitis C virus; HR, hazard ratio; PLT, platelets.

hypovascular hypointense nodules to typical HCC was reported as 10–17%/year,[9,10] which is comparable to the present study. Typical HCC arose exclusively among the nodules of 8 mm or more, as in previous studies in which the larger hypovascular hypointense nodules were found to be the risk factor for progression to typical HCC in the initial MRI study.[9,10]

Hyperintensity on T2WI[12] or diffusion-weighted images (DWI)[11] also was reported to be useful for prediction of typical HCC progress in hypovascular hypointense nodules. In our patients, none of the nodules in the non-clean liver group showed hyperintensity on T2WI, suggesting that the hepatocyte phase is more sensitive for detecting the early stage of hepatocarcinogenesis.[15] DWI were not evaluated in this study because this usually detects pathologically advanced HCC of larger size or with hypervascularity.[23] Thus, it is reasonable that the hepatocyte phase can effectively recognize the earliest stage of HCC development without T2WI or DWI.

In 11 of 17 patients, typical HCC developed at sites other than the initially detected hypovascular hypointense nodules. As shown in Figure 3, the incidence rates of such HCC in the non-clean liver group was significantly higher than in the clean liver group ($P = 0.003$), indicating that a non-clean liver itself is a risk factor for HCC development, apart from the detectable hypovascular hypointense nodules. In addition, in four patients with nodules even below 8 mm, two developed HCC at different sites from the initial nodules during follow up (data not shown). Taken together, a non-clean liver has the higher potential for hepatocarcinogenesis or for undetectable precursor lesions. The non-clean liver may reflect more advanced genetic or epigenetic changes in the background hepatocytes, however, the detailed biological mechanism is not clear in this study.

Non-clean liver was an independent risk factor for the development of typical HCC, apart from well-documented risk factors (Table 2), such as cirrhosis,[24] ALT,[25] γ-GT,[26] age and AFP.[27] A non-clean liver is a significant risk for HCC development also for those without cirrhosis or with high platelet counts (Fig. 4). This means patients at increased risk of HCC development can be discerned as having a non-clean liver even among low-risk subgroups.

Conversely, patients without such nodules (clean liver group) showed a significantly lower risk of developing typical HCC than those with non-clean livers (0.0% vs 11.1% at 1 year, 6.8% vs 55.5% at 3 years of follow up; $P < 0.001$), suggesting that gadoxetic acid-enhanced MRI could detect precursor lesions sensitively enough to rule out immediate (within 1 year) development of typical HCC. Although seven patients in the clean liver group developed typical HCC only after 1 year, these patients had other risk factors for HCC development, including lower platelet counts, implying more advanced liver cirrhosis or high AFP (data not shown). Such HCC may arise from precursor lesions that cannot be visualized by current imaging techniques.

This study is a retrospective study and has some limitations. We included patients with HBV and HCV together, because gadoxetic acid-enhanced MRI findings or HCC development do not differ between these two groups and HBV or HCV infection is not an independent risk factor for typical HCC development. However, the number of HBV patients was too small ($n = 26$) to statistically confirm the current result when limited to HBV patients only. Prospective studies with larger numbers of patients who have uniform liver disease etiologies and imaging intervals are needed to verify our findings in different settings. Although the imaging interval of the non-clean liver group was shorter than the clean liver group (3 vs 4 months: $P = 0.015$), the median intervals between the initial MRI and HCC diagnosis was 16 months in the non-clean liver group and 21 months in the clean liver group. They are short enough for cumulative detection of HCC development for 3 years and it is assumed that there was little influence on the conclusions.

In conclusion, patients with chronic viral liver disease are at high risk for developing typical HCC at any sites of the liver if they have hypovascular hypointense nodules on gadoxetic acid-enhanced MRI. These patients should be closely followed up for developing typical HCC not only at the same site but also at different sites from the initial nodule.

REFERENCES

1 Ichikawa T, Saito K, Yoshioka N *et al.* Detection and characterization of focal liver lesions: a Japanese phase III, multicenter comparison between gadoxetic acid disodium-enhanced magnetic resonance imaging and contrast-enhanced computed tomography predominantly in patients with hepatocellular carcinoma and chronic liver disease. *Invest Radiol* 2010; **45**: 133–41.
2 Halavaara J, Breuer J, Ayuso C *et al.* Liver tumor characterization: comparison between liver-specific gadoxetic acid disodium-enhanced MRI and biphasic CT – a multicenter trial. *J Comput Assist Tomogr* 2006; **30**: 345–54.
3 Hamm B, Staks T, Muhler A *et al.* Phase I clinical evaluation of Gd-EOB-DTPA as a hepatobiliary MR contrast

agent: safety, pharmacokinetics, and MR imaging. *Radiology* 1995; **195**: 785–92.
4 Hammerstingl R, Huppertz A, Breuer J *et al.* European EOB-study group. Diagnostic efficacy of gadoxetic acid (Primovist)-enhanced MRI and spiral CT for a therapeutic strategy: comparison with intraoperative and histopathologic findings in focal liver lesions. *Eur Radiol* 2008; **18**: 457–67.
5 Huppertz A, Balzer T, Blakeborough A *et al.* European EOB Study Group. Improved detection of focal liver lesions at MR imaging: multicenter comparison of gadoxetic acid-enhanced MR images with intraoperative findings. *Radiology* 2004; **230** (1): 266–75.
6 Di Martino M, Marin D, Guerrisi A *et al.* Intraindividual comparison of gadoxetate disodium-enhanced MR imaging and 64-section multidetector CT in the detection of hepatocellular carcinoma in patients with cirrhosis. *Radiology* 2010; **256**: 806–16.
7 Inoue T, Kudo M, Komuta M *et al.* Assessment of Gd-EOB-DTPA-enhanced MRI for HCC and dysplastic nodules and comparison of detection sensitivity versus MDCT. *J Gastroenterol* 2012; **47**: 1036–47.
8 Golfieri R, Renzulli M, Lucidi V, Corcioni B, Trevisani F, Bolondi L. Contribution of the hepatobiliary phase of Gd-EOB-DTPA-enhanced MRI to dynamic MRI in the detection of hypovascular small (</= 2 cm) HCC in cirrhosis. *Eur Radiol* 2011; **21**: 1233–42.
9 Kumada T, Toyoda H, Tada T *et al.* Evolution of hypointense hepatocellular nodules observed only in the hepatobiliary phase of gadoxetate disodium-enhanced MRI. *AJR Am J Roentgenol* 2011; **197** (1): 58–63.
10 Motosugi U, Ichikawa T, Sano K *et al.* Outcome of hypovascular hepatic nodules revealing no gadoxetic acid uptake in patients with chronic liver disease. *J Magn Reson Imaging* 2011; **34** (1): 88–94.
11 Kim YK, Lee WJ, Park MJ, Kim SH, Rhim H, Choi D. Hypovascular hypointense nodules on hepatobiliary phase gadoxetic acid-enhanced MR images in patients with cirrhosis: potential of DW imaging in predicting progression to hypervascular HCC. *Radiology* 2012; **265** (1): 104–14.
12 Hyodo T, Murakami T, Imai Y *et al.* Hypovascular nodules in patients with chronic liver disease: risk factors for development of hypervascular hepatocellular carcinoma. *Radiology* 2013; **266**: 480–90.
13 Bartolozzi C, Battaglia V, Bargellini I *et al.* Contrast-enhanced magnetic resonance imaging of 102 nodules in cirrhosis: correlation with histological findings on explanted livers. *Abdom Imaging* 2013; **38**: 290–6.
14 Golfieri R, Grazioli L, Orlando E *et al.* Which is the best MRI marker of malignancy for atypical cirrhotic nodules: hypointensity in hepatobiliary phase alone or combined with other features? Classification after Gd-EOB-DTPA administration. *J Magn Reson Imaging* 2012; **36**: 648–57.
15 Sano K, Ichikawa T, Motosugi U *et al.* Imaging study of early hepatocellular carcinoma: usefulness of gadoxetic acid-enhanced MR imaging. *Radiology* 2011; **261**: 834–44.
16 Motosugi U. Hypovascular hypointense nodules on hepatocyte phase gadoxetic acid-enhanced MR images: too early or too progressed to determine hypervascularity. *Radiology* 2013; **267** (1): 317–8.
17 Asayama Y, Yoshimitsu K, Nishihara Y *et al.* Arterial blood supply of hepatocellular carcinoma and histologic grading: radiologic-pathologic correlation. *AJR Am J Roentgenol* 2008; **190** (1): W28–34.
18 Motosugi U, Ichikawa T, Sou H *et al.* Liver parenchymal enhancement of hepatocyte-phase images in Gd-EOB-DTPA-enhanced MR imaging: which biological markers of the liver function affect the enhancement? *J Magn Reson Imaging* 2009; **30**: 1042–6.
19 Bruix J, Sherman M, American Association for the Study of Liver Diseases. Management of hepatocellular carcinoma: an update. *Hepatology* 2011; **53**: 1020–2.
20 Motosugi U, Ichikawa T, Araki T. Rules, roles, and room for discussion in gadoxetic acid-enhanced magnetic resonance liver imaging: current knowledge and future challenges. *Magnetic Rsonance in Medical Sciences.* 2013; **12**: 161–75.
21 Kitao A, Zen Y, Matsui O *et al.* Hepatocellular carcinoma: signal intensity at gadoxetic acid-enhanced MR imaging – correlation with molecular transporters and histopathologic features. *Radiology* 2010; **256**: 817–26.
22 Narita M, Hatano E, Arizono S *et al.* Expression of OATP1B3 determines uptake of Gd-EOB-DTPA in hepatocellular carcinoma. *J Gastroenterol* 2009; **44**: 793–8.
23 Nasu K, Kuroki Y, Tsukamoto T, Nakajima H, Mori K, Minami M. Diffusion-weighted imaging of surgically resected hepatocellular carcinoma: imaging characteristics and relationship among signal intensity, apparent diffusion coefficient, and histopathologic grade. *American Journal of Roentgenology* 2009; **193**: 438–44.
24 Degos F, Christidis C, Ganne-Carrie N *et al.* Hepatitis C virus related cirrhosis: time to occurrence of hepatocellular carcinoma and death. *Gut* 2000; **47** (1): 131–6.
25 Tarao K, Rino Y, Ohkawa S *et al.* Association between high serum alanine aminotransferase levels and more rapid development and higher rates of incidence of hepatocellular carcinoma in patients with hepatitis C virus-associated cirrhosis. *Cancer* 1999; **86**: 589–95.
26 Ikeda K, Saitoh S, Suzuki Y *et al.* Disease progression and hepatocellular carcinogenesis in patients with chronic viral hepatitis: a prospective observation of 2215 patients. *J Hepatol* 1998; **28**: 930–8.
27 Ikeda K, Saitoh S, Koida I *et al.* A multivariate analysis of risk factors for hepatocellular carcinogenesis: a prospective observation of 795 patients with viral and alcoholic cirrhosis. *Hepatology* 1993; **18** (1): 47–53.

Amphipathic α-Helices in Apolipoproteins Are Crucial to the Formation of Infectious Hepatitis C Virus Particles

Takasuke Fukuhara[1#], Masami Wada[1#], Shota Nakamura[2], Chikako Ono[1], Mai Shiokawa[1], Satomi Yamamoto[1], Takashi Motomura[1], Toru Okamoto[1], Daisuke Okuzaki[3], Masahiro Yamamoto[4], Izumu Saito[5], Takaji Wakita[6], Kazuhiko Koike[7], and Yoshiharu Matsuura[1*]

[1]Department of Molecular Virology, [2]Department of Infection Metagenomics, [3]DNA-Chip Developmental Center for Infectious Diseases, [4]Department of Immunoparasitology, Research Institute for Microbial Diseases, Osaka University, Osaka, Japan, [5]Laboratory of Molecular Genetics, Institute of Medical Science, The University of Tokyo, Tokyo, Japan, [6]Department of Virology II, National Institute of Infectious Diseases, Tokyo, Japan, and [7]Department of Gastroenterology, Graduate School of Medicine, The University of Tokyo, Tokyo, Japan.

[#]These authors equally contributed to this work.
*Corresponding author:
Yoshiharu Matsuura, DVM, PhD
Department of Molecular Virology
Research Institute for Microbial Diseases, Osaka University
3-1, Yamada-oka, Suita, Osaka 565-0871, Japan
E-mail: matsuura@biken.osaka-u.ac.jp
Tel: 81-6-6879-8340

Fax: 81-6-6879-8269

Running title: Exchangeable apolipoproteins in HCV assembly
Keywords: HCV assembly, apolipoproteins, amphipathic α-helix

Abstract

Apolipoprotein B (ApoB) and ApoE have been shown to participate in the particle formation and the tissue tropism of hepatitis C virus (HCV), but their precise roles remain uncertain. Here we show that amphipathic α-helices in the apolipoproteins participate in the HCV particle formation by using zinc finger nucleases-mediated apolipoprotein B (ApoB) and/or ApoE gene knockout Huh7 cells. Although Huh7 cells deficient in either ApoB or ApoE gene exhibited slight reduction of particles formation, knockout of both ApoB and ApoE genes in Huh7 (DKO) cells severely impaired the formation of infectious HCV particles, suggesting that ApoB and ApoE have redundant roles in the formation of infectious HCV particles. cDNA microarray analyses revealed that ApoB and ApoE are dominantly expressed in Huh7 cells, in contrast to the high level expression of all of the exchangeable apolipoproteins, including ApoA1, ApoA2, ApoC1, ApoC2 and ApoC3 in human liver tissues. The exogenous expression of not only ApoE, but also other exchangeable apolipoproteins rescued the infectious particle formation of HCV in DKO cells. In addition, expression of these apolipoproteins facilitated the formation of infectious particles of genotype 1b and 3a chimeric viruses. Furthermore, expression of amphipathic α-helices in the exchangeable apolipoproteins facilitated the particle formation in DKO cells through an interaction with viral particles. These results suggest that amphipathic α-helices in the exchangeable apolipoproteins play crucial roles in the infectious particle formation of HCV and provide clues to the understanding of life cycle of HCV and the development of novel anti-HCV therapeutics targeting for viral assembly.

Author Summary

In vitro systems have been developed for the study of hepatitis C virus (HCV) infection and have revealed many details of the life cycle of HCV. Apolipoprotein B (ApoB) and ApoE have been shown to play crucial roles in the particle formation of HCV, based on data obtained by siRNA-mediated gene knockdown and overexpression of the proteins. However, precise roles of the apolipoproteins in HCV assembly have not been elucidated yet. In this study, we show that infectious particle formation of HCV in Huh7 cells was severely impaired by the knockout of both ApoB and ApoE genes by artificial nucleases, and this reduction was cancelled by the expression of not only ApoE, but also other exchangeable apolipoproteins, including ApoA1, ApoA2, ApoC1, ApoC2 and ApoC3. In addition, expression of amphipathic α-helices in the exchangeable apolipoproteins restored the infectious particle formation in the double-knockout cells through an interaction with viral particles. These results provide clues to the understanding of life cycle of HCV and the development of novel antivirals to HCV.

Introduction

More than 160 million individuals worldwide are infected with hepatitis C virus (HCV), and cirrhosis and hepatocellular carcinoma induced by HCV infection are life-threatening diseases (1). Current standard therapy combining peg-interferon (IFN), ribavirin (RBV) and a protease inhibitor has achieved a sustained virological response (SVR) in over 80% of individuals infected with HCV genotype 1 (2). In addition, many antiviral agents targeting non-structural proteins and host factors involved in HCV replication have been applied in clinical trials (3, 4).

In vitro systems have been developed for the study of HCV infection and have revealed many details of the life cycle of HCV. By using pseudotype particles bearing HCV envelope proteins and RNA replicon systems, many host factors required for entry and RNA replication have been identified, respectively (5, 6). In addition, development of a robust *in vitro* propagation system of HCV based on the genotype 2a JFH1 strain (HCVcc) has gradually clarified the mechanism of assembly of HCV particles (7, 8). It has been shown that the interaction of NS2 protein with structural and non-structural proteins facilitates assembly of the viral capsid and formation of infectious particles at the connection site between the ER membrane and the surface of lipid droplets (LD) (9). On the other hand, very low density lipoprotein (VLDL) associated proteins, including apolipoprotein B (ApoB), ApoE, and microsomal triglyceride transfer protein (MTTP), have been shown to play crucial roles in the formation of infectious HCV particles (10-12). Generally, ApoA, ApoB, ApoC and ApoE bind the surface of lipoprotein through the interaction between amphipathic α-helices and ER-derived membrane (13,14). This binding of apolipoproteins enhances the stability and hydrophilicity of lipoprotein. However, the specific roles played by the apolipoproteins in HCV particle formation are controversial. Gastaminza et al. demonstrated that ApoB and MTTP are cellular factors essential for an efficient assembly of infectious HCV particles (10). However, studies by other groups demonstrated that ApoE is a major determinant of the infectivity and particle formation of HCV, and the ApoE fraction is highly enriched with infectious particles (11). In addition, Mancone et al. showed that ApoA1 is required for production of infectious particles of HCV (15). However, the evidence of the involvement of apolipoproteins in HCV particle formation is dependent on knockdown data and exogenous expression of the apolipoproteins, and thus the precise mechanisms of participation of the apolipoproteins in HCV assembly have not been elucidated (10, 11, 16).

Recently, several novel genome editing techniques have been developed, including methods using zinc finger nucleases (ZFN), transcription activator like-effector nucleases (TALEN) and CRISPR/Cas9 systems (17-19). DNA double strand breaks (DSBs) induced by these artificial nucleases can be repaired by error-prone non-homologous end joining (NHEJ), resulting in mutant mice or cell lines carrying deletions, insertions, or substitutions at the cut site. To clarify the detailed function of gene family with redundant functions, the generation of animals or cell lines carrying multiple mutated genes may be essential.

In this study, Huh7 cell lines deficient in both ApoB and ApoE genes were established by using ZFNs and revealed that ApoB and ApoE redundantly participate in the formation of infectious HCV particles. Interestingly, the expression of other exchangeable apolipoproteins, i.e., ApoA1, ApoA2, ApoC1, ApoC2 and ApoC3, facilitated HCV assembly in ApoB and ApoE double-knockout cells. In addition, the expression of amphipathic α-helices in the exchangeable apolipoproteins restored the production of infectious particles in the double-knockout cells through an interaction with viral particles.

Results

Several apolipoproteins participate in the production of infectious viral particles. First, we compared expression levels of apolipoproteins between hepatocyte and hepatic cancer cell lines including Huh7 and HepG2 cells (Figure 1A and B). The web-based search engine NextBio (NextBio, Santa Clara, CA) revealed that ApoB, ApoH and the exchangeable apolipoproteins

ApoA1, ApoA2, ApoC1, ApoC2, ApoC3, and ApoE are highly expressed in human liver tissues (Figure 1A). On the other hand, the expressions of ApoA1, ApoC1, ApoC2, ApoC3 and ApoH in hepatic cancer cell lines were suppressed compared to those in hepatocytes (Figure 1B). To examine the roles of apolipoproteins in the formation of infectious HCV particles, the effects of knockdown of ApoA2, ApoB and ApoE on the infectious particle production in the supernatants were determined in Huh7 cells by focus forming assay (Figure 1C). The transfection of siRNAs targeting to ApoA2, ApoB and ApoE significantly suppressed the production of infectious HCV particles. This inhibitory effect is well consistent with the high level of expression of these apolipoproteins in the hepatic cancer cell lines, suggesting that the apolipoproteins involved in HCV assembly are dependent on the expression pattern in hepatic cancer cell lines, including Huh7 cells (20). Therefore, we examined the effects of exogenous expression of the apolipoproteins highly expressed in the liver tissues on the infection of HCV in the stable ApoE-knockdown Huh7 cells (Figure 1D). In contrast to the control-knockdown cells, expression of not only ApoE but also ApoA1, ApoA2, and ApoC1 rescued the infectious particle formation in the ApoE-knockdown cells (Figure 1E), suggesting that various exchangeable apolipoproteins participate in the efficient production of infectious HCV particles.

ApoB and ApoE have a redundant role in HCV particle formation. To obtain more convincing data on the involvement of apolipoproteins in the production of infectious HCV particles, we established knockout (KO) Huh7 cells deficient in either ApoB (B-KO1 and B-KO2) or ApoE (E-KO1 and E-KO2) by using ZFN (Figure S1). Deficiencies of ApoB or ApoE expression in these cell lines were confirmed by ELISA and immunoblotting analyses (Figure S1). First, we examined the roles of ApoB and ApoE on the entry and RNA replication of HCV by using HCV pseudotype particles (HCVpp) and subgenomic replicon (SGR) of the JFH1 strain, respectively. The B-KO and E-KO cell lines exhibited no significant effect on the infectivity of HCVpp and the colony formation of SGR (Figure S2A and B), suggesting that ApoB and ApoE are not involved in the entry and replication processes of HCV. To examine the role of ApoB and ApoE in the propagation of HCV, HCVcc was inoculated into parental, B-KO and E-KO cell lines at an MOI of 1, and intracellular viral RNA and infectious titers in the supernatants were determined (Figure S2C and D). Although RNA replication and infectious particle formation in B-KO cells upon infection with HCV were comparable with those in parental Huh7 cells, E-KO cells exhibited slight reduction of particle formation, and the expression of ApoE in E-KO cells rescued infectious particle formation (Figure S2C-E). Next, to examine the redundant role of ApoB, the effect of knockdown of ApoB on HCV assembly was determined in parental and E-KO Huh7 cell lines (Figure 2A). Knockdown of ApoB in E-KO cells resulted in a more efficient reduction of infectious particle production than that in parental Huh7 cells, suggesting that ApoB and ApoE have a redundant role in the formation of infectious HCV particles.

To further confirm the redundant role of ApoB and ApoE in the HCV life cycle, especially in the particle formation, 2 clones of ApoB and ApoE double-knockout (BE-KO1 and BE-KO2) Huh7 cells were established by ZFNs (Figure S3A and B). The lack of ApoB and ApoE expressions was confirmed by immunoblotting and ELISA analyses (Figure S3C-E). The BE-KO cell lines also exhibited no significant effect on the infectivity of HCVpp (Figure 2B) and the colony formation of SGR (Figure 2C). Next, we examined the redundant role of ApoB and ApoE on the propagation of HCVcc. Upon infection with HCVcc at an MOI of 1, infectious titers in the supernatants of BE-KO1 and BE-KO2 cells were 50 to 100 times lower than those of parental Huh7 cells at 72 h post-infection, while the level of intracellular RNA replication was comparable (Figure 2D and E). In addition, exogenous expression of ApoE in BE-KO (ApoE-res) cells rescued the production of infectious viral particles to levels comparable to those in parental Huh7 cells (Figure 2F and G), suggesting that ApoB and ApoE redundantly participate in the particle formation of HCV.

MTTP participates in HCV particle formation through the maturation of ApoB. It is difficult to determine the roles of ApoB in the particle formation of HCV, because ApoB is too large (550

kDa) to obtain cDNA for expression. However, previous reports have shown that expression of MTTP facilitates the secretion of ApoB (21). To further clarify the roles of ApoB in the life cycle of HCV, we established knockout Huh7 cell lines deficient in MTTP (M-KO1 and M-KO2) and in both ApoE and MTTP (EM-KO1 and EM-KO2) by using the ZFN and CRISPR/Cas9 system (Figure S4A and E). The lack of MTTP, ApoB and ApoE expressions was confirmed by immunoblotting and ELISA analyses (Figure S4B-D and F-H). As previously reported, the secretion of ApoB was completely abrogated in M-KO and EM-KO cells, while the mRNA levels of ApoB were comparable among Huh7, M-KO and EM-KO cells (Figure S4I). To examine the roles of MTTP in the assembly of HCV through the secretion of ApoB, HCVcc was inoculated into the Huh7, B-KO, M-KO, E-KO, BE-KO and EM-KO cell lines at an MOI of 1, and intracellular HCV genomes and infectious titers in the supernatants were determined (Figure 3A-C). Although intracellular RNA replication in M-KO and EM-KO cells was comparable with that in Huh7, B-KO, E-KO and BE-KO cells (Figure 3B), infectious titers in the supernatants of EM-KO cells were severely impaired as seen in BE-KO cells, while those of M-KO cells were comparable to those of parental Huh7cells (Figure 3C), suggesting that MTTP participates in the HCV assembly through the regulation of ApoB secretion. To further confirm the roles of MTTP in HCV assembly through ApoB secretion, the effects of exogenous expression of MTTP in EM-KO cells on the infectious particle formation of HCV were determined. Immunoblotting and ELISA analyses revealed that exogenous expression of MTTP rescued the secretion of ApoB into the supernatants of EM-KO cells (Figure 3D and E), while expression of ApoE or MTTP in both BE-KO and EM-KO cells exhibited no effect on the intracellular RNA replication (Figure 3F). Although exogenous expression of ApoE rescued the infectious particle formation of HCV in both BE-KO and EM-KO cells, expression of MTTP rescued the particle formation in EM-KO cells but not in BE-KO cells (Figure 3G), supporting the notion that MTTP plays a crucial role in the HCV assembly through the maturation of ApoB.

Exchangeable apolipoproteins redundantly participate in the assembly of infectious HCV particles. Next, to examine the roles played in HCV particles formation by other apolipoproteins highly expressed in the liver (Figure 1A), the expressions of ApoA1, ApoA2, ApoC1, ApoC2, ApoC3 and ApoH in BE-KO1 cells were suppressed by siRNAs (Figure 4A and S5). While knockdown of ApoA1, ApoC3 and ApoH exhibited no effect, that of ApoA2, ApoC1 and ApoC2 significantly inhibited the release of infectious particles, which was consistent with the expression pattern of endogenous apolipoproteins except for ApoH in Huh7 cells (Figure 1B), suggesting that not only ApoB and ApoE but also other exchangeable apolipoproteins participate in HCV particle formation. To confirm the redundant role of these apolipoproteins on the infectious particle formation, the effects of exogenous expression of these apolipoproteins on the propagation of HCVcc in BE-KO1 cells were determined. ApoA1, ApoA2, ApoC1, ApoC2, ApoC3, ApoE and ApoH were expressed by lentiviral vector in BE-KO1 cells (Figure 4B upper panel). The expressions of ApoA1, ApoA2, ApoC1, ApoC2, ApoC3 and ApoE but not of ApoH enhanced extracellular HCV RNA, while they exhibited no effect on intracellular HCV RNA (Figure 4C). In addition, the expressions of these exchangeable apolipoproteins enhanced the infectious particle formation in the supernatants of BE-KO1 cells (Figure 4B lower panel). On the other hand, the expression of nonhepatic apolipoproteins, including ApoD, ApoL1, and ApoO, exhibited no effect on HCV particle formation in BE-KO1 cells (Figure S6). These results suggest that exogenous expression of not only the ApoE but also the ApoA and ApoC families can compensate for the impairment of HCV particle formation in BE-KO1 cells. Interestingly, specific infectivity (infectious titers / viral RNA levels in supernatants) was also enhanced by the expression of ApoA1, ApoA2, ApoC1, ApoC2, ApoC3 and ApoE, suggesting that these apolipoproteins participate in the infectious but not non-infectious particle formation of HCV (Figure 4D). Previous reports have suggested that the expressions of Claudin1 (CLDN1), miR-122 and ApoE facilitate the production of infectious particles in nonhepatic 293T cells (16). Therefore, the effects of exogenous expression of

exchangeable apolipoproteins on particle formation were examined in 293T cells expressing CLDN1 and miR-122 (293T-CLDN/miR-122 cells). Exogenous expression of ApoA1, ApoA2, ApoC1, ApoC2, ApoC3 and ApoE, but not of ApoH by lentiviral vector facilitated the production of infectious HCV particles in 293T-CLDN/miR-122 cells (Figure 4E). On the other hand, the expression of ApoE exhibited no effect on the propagation of Japanese encephalitis virus (JEV) and dengue virus (DENV) (Figure S7) in BE-KO1 cells. These results suggest that the exchangeable apolipoproteins and ApoB redundantly and specifically participate in the formation of HCV particles.

To examine the role of exchangeable apolipoproteins in the formation of other genotypes of HCV, the effect of exogenous expression of these apolipoproteins on the propagation of genotype 1b and 3a chimeric HCVcc, TH/JFH1 and S310/JFH1 viruses in BE-KO1 cells was determined (Figure 5) (22, 23). As seen in infection with HCVcc (JFH1), expression of ApoA1, ApoA2, ApoC1, ApoC2, ApoC3 and ApoE enhanced the formation of infectious particles of TH/JFH1 and S310/JFH1 chimeric viruses. These results suggest that ApoA1, ApoA2, ApoC1, ApoC2, ApoC3 and ApoE redundantly participate in the efficient formation of infectious HCV particles of genotypes 1b, 2a and 3a.

Apolipoproteins participate in the post-envelopment step of particle formation. To determine the details of the assembly of infectious HCV particles in the BE-KO1 cells, intracellular infectious titers were determined in Huh7, BE-KO1 and ApoE-res cells by using the freeze and thaw method. Not only intracellular but also extracellular infection titers were impaired in BE-KO1 cells compared with those in parental and ApoE-res cells (Figure 6A), suggesting that intracellular particle formation is impaired by deficiencies in the expression of ApoB and ApoE. Previous reports have shown that the recruitment of viral proteins around LD and redistribution of LD are essential for HCV assembly (24). To clarify the roles of the exchangeable apolipoproteins on HCV assembly in more detail, we examined the intracellular localization of viral proteins, LD and ER in BE-KO1 and ApoE-res cells. The localization of core proteins around LD and the membranous-web structure forming the replication complex were observed in BE-KO1 cells upon infection with HCVcc, as reported in parental Huh7 cells (Figure 6B, 6C and S8). However, greater accumulation of core proteins and LD around the perinuclear region was detected in BE-KO1 cells in comparison with ApoE-res cells (Figure 6C and 6D), supporting the notion that apolipoproteins participate in the infectious particle formation in HCV rather than viral RNA replication. Previous studies revealed that core proteins were mainly localized on the ER membrane upon infection with the genotype 2a Jc1 strain-based HCVcc (HCVcc/Jc1), and inhibition of capsid assembly and envelopment caused accumulation of core proteins on the surface of LD (25-27). In ApoE-res cells, core proteins of HCVcc/Jc1 were mainly localized on the ER membrane, in contrast to the co-localization of core proteins of HCVcc (JFH1) with LD (Figure 6E upper). However, core proteins were accumulated around LD in BE-KO1 cells infected with HCVcc/Jc1, as seen in those infected with HCVcc (JFH1) (Figure 6E lower). These results suggest that apolipoproteins participate in the steps of HCV particle formation occurring after HCV protein assembly on the LD.

To further examine the involvement of apolipoproteins in the infectious particle formation of HCV, culture supernatants and cell lysates of BE-KO1 and ApoE-res cells infected with HCVcc were analyzed by buoyant density ultracentrifugation (Figure 7A-B) (28). Secretion of viral capsids in the supernatants was severely impaired in BE-KO1 cells in comparison with that in ApoE-res cells (Figure 7A upper), in contrast to the detection of abundant intracellular capsids in both cell lines (Figure 7B upper). Although peak levels of the core proteins and infectious titers were detected around 1.08 g/ml in both cell lines, the infectious titers in all fractions of BE-KO1 cells were significantly lower than those in ApoE-res cells, supporting the notion that apolipoproteins participate in the post-assembly process of HCV capsids which is required to confer infectivity. Next, to examine the involvement of apolipoproteins in the envelopment of HCV particles, lysates of BE-KO1 and ApoE-res cells infected with HCVcc were treated with proteinase K in the presence or

absence of Triton X (26). Protection of HCV core proteins from the protease digestion was observed in both cell lysates (Figure 7C), suggesting that apolipoproteins are not involved in the envelopment of HCV particles. Collectively, these results suggest that exchangeable apolipoproteins participate in the post-envelopment step of HCV particle formation.

Amphipathic α-helices in exchangeable apolipoproteins participate in the formation of infectious HCV particles through the interaction with viral particles. To determine the structural relevance of apolipoproteins involved in the HCV assembly, the secondary structures of the apolipoproteins were deduced by using a CLC Genomics Workbench and previous reports (Figure 8A) (29-34). Tandem repeats of amphipathic α-helices were observed in the apolipoproteins capable of rescuing HCV assembly in BE-KO1 cells, but not in those lacking this activity, suggesting that amphipathic α-helices in the apolipoproteins participate in the assembly of HCV. To examine the involvement of the amphipathic α-helices of the exchangeable apolipoproteins in the particle formation of HCV, we constructed expression plasmids encoding deletion mutants of ApoE and ApoC1, and then these deletion mutants were exogenously expressed in BE-KO1 cells by lentiviral vectors (Figure 8B and C upper panels). The expression of all of the deletion mutants of ApoE and ApoC1 containing either N-terminal or C-terminal amphipathic α-helices rescued the particle formation of HCV in BE-KO1 cells (Figure 8B and C lower panels), suggesting that amphipathic α-helices in the apolipoproteins play crucial roles in the production of infectious HCV particles. In addition, more abundant full-length and truncated ApoE were detected in the precipitates of the culture supernatants of cells infected with HCVcc than those of mock-infected cells concentrated by ultracentrifugation, suggesting that the amphipathic α-helices of apolipoproteins are directly associated with HCV particles (Figure 8D and E). Taken together, the data in this study strongly suggest that exchangeable apolipoproteins redundantly participate in the infectious particle formation of HCV through the interaction between amphipathic α-helices and viral particles.

Discussion

In this study, we demonstrated the redundant roles of ApoB and the exchangeable apolipoproteins ApoA1, ApoA2, ApoC1, ApoC2, ApoC3 and ApoE in the assembly of infectious HCV particles. The deficiencies of both ApoB and ApoE inhibited the production of infectious HCV particles in Huh7 cells, and exogenous expression of exchangeable apolipoproteins rescued the particle formation. cDNA microarray revealed that the expression patterns of exchangeable apolipoproteins in hepatic cancer cell lines are widely different from those in liver tissue. In previous reports, ApoE and ApoB were identified as important host factors for the assembly of infectious HCV particles (10, 11), and knockdown of ApoE and ApoB expression also inhibited the production of infectious particles in this study. Because ApoB and ApoE are major apolipoproteins in VLDL, several reports have suggested that the VLDL production machinery participates in the production of HCV particles. Furthermore, density gradient analyses revealed co-fractionation of HCV RNA with lipoproteins, with the resulting complexes being termed lipoviroparticles (LVP) (12, 35). However, it has been reported that there is no correlation between secretion of VLDL and production of LVP (36). In addition, exogenous expression of ApoE facilitated the infectious particle formation of HCV in 293T cells stably expressing CLDN1 and miR-122 (16), suggesting that ApoE-mediated particle formation is independent from VLDL production. Furthermore, exogenous expression of ApoA1, a major apolipoprotein of HDL, also facilitated the production of HCV particles as shown in Figure 4E. These data suggest that the roles of the exchangeable apolipoproteins in HCV assembly are independent from the production of VLDL. MTTP plays crucial roles in the lipoprotein formation through the incorporation of triglyceride into growing lipoprotein and secretion of ApoB (21). Although it has been shown that treatment with an MTTP inhibitor impairs the production of HCV particles (11), in this study, we found that knockout of MTTP abrogated the secretion of ApoB but not the production of infectious HCV particles. Collectively, these data suggest that exchangeable apolipoproteins redundantly participate in the infectious particle formation of HCV independently

from lipoprotein secretion machinery.

Production of HCV capsids in the culture supernatants is impaired in 293T cells expressing miR-122 due to lack of ApoE expression, but envelopment of viral capsids is observed (37), suggesting that ApoE is involved in the post-envelopment step. Coller et al. suggested that ApoE is associated with *de novo* formation of HCV particles during secretory pathway based on an experiment using HCV possessing a tetracysteine-tag in the core protein (38). In this study, ApoA1, ApoA2, ApoC1, ApoC2, ApoC3 and ApoE enhanced the formation of HCV particles in the post-envelopment step. These results suggest that a direct interaction between exchangeable apolipoproteins and enveloped particles in the ER lumen facilitates an efficient secretion of infectious HCV particles. Ultrastructural analysis of HCV particles has shown that large amounts of apolipoproteins, including ApoA1, ApoB and ApoE, bind to the surface of viral particles (39). Interestingly, ApoE-specific antibodies were more efficient in capturing viral particles than α-E1/E2 antibodies, and significantly large numbers of gold particles reacting with ApoE were observed per virion than those with E2, suggesting that viral envelope proteins are masked by a large amount of apolipoproteins. The unique characteristics of interaction between apolipoproteins and HCV particles might be applied for visualization of entry and purification of HCV particles by using GFP- or affinity-tagged amphipathic α-helices of apolipoproteins. In the previous report, virocidal amphipathic helical peptides impaired the infectivity of viral particles (40). There is a possibility that such peptide influences on the interaction between apolipoproteins and viral particles, and might be a new therapeutic approach.

In previous reports, the importance of the interaction between lipoprotein receptors and ApoE in the entry of HCV has been well established. Lipoprotein receptors including scavenger receptor class B type 1 (SR-B1) and low-density lipoprotein receptor (LDLR) are involved in HCV entry into the target cells (41, 42). LDLR is thought to mediate cell attachment of HCV through an interaction with virus associated ApoE (43, 44). SR-B1 also interacts with ApoE and hypervariable region 1 (HVR1) in the envelope protein of HCV (43). In this study we have shown that exchangeable apolipoproteins including not only ApoE but also ApoA and ApoC facilitate the production of infectious HCV particles, and that exchangeable apolipoproteins directly associate with viral particles. Meunier et al. reported that ApoC1 associates intracellularly with viral particles during particle morphogenesis and enhances the entry of HCV through an interaction of the C-terminal region of ApoC1 with heparan sulfate (45). Another group also showed that ApoC1 enhances HCV infection through the triple interplay among HVR1, ApoC1, and SR-B1 (46). These results suggest that the interaction of HCV particles with apolipoproteins also participates in the entry through the binding of lipoprotein receptors including SR-B1 and LDLR.

Although the gene-knockout technique is essential to obtain reproducible and reliable data, and many knockout mice have been produced in various research areas, the development of experimental tools for HCV study has also been hampered by the narrow cell tropism (47, 48). A humanized mouse model in which human liver cells were xenotransplanted into immunodeficient mouse was developed and provided an important platform for the analysis of pathogenesis and the development of antivirals for HCV (49). However, the exogenous expression of human receptor molecules required for HCV entry and impairment of innate immunity are required for the complete propagation of HCV in mice (50). Gene-knockout techniques using a CRISPR/Cas9 system composed of guide RNA and Cas9 nuclease that form RNA-protein complexes to cleave the target sequences (19) have allowed quick and easy establishment of gene-knockout mice and cancer cell lines (51, 52), and indeed, such MTTP-knockout cell lines were established also in this study. Recently, the high-throughput screening of host factors involved in several conditions was reported by using a CRISPR/Cas9 system (53). Together, these novel genome-editing techniques are expected to reveal the precise roles of host factors involved in the HCV life cycle.

In summary, we have shown that apolipoproteins, including ApoA1, ApoA2, ApoC1, ApoC2, ApoC3, ApoE and ApoB, possess redundant roles in the assembly of HCV through the interaction of

363 the amphipathic α-helices in the apolipoproteins with viral particles in the post-envelopment step. It
364 is hoped that these findings will provide clues to the life cycle of HCV and assist in the development
365 of novel antivirals targeting the assembly process of HCV.
366
367 **Materials and Methods**
368 **NextBio Body Atlas.** The NextBio Body Atlas application presents an aggregated analysis of gene
369 expression across various normal tissues, normal cell types, and cancer cell lines (20). It enables us to
370 investigate the expression of individual genes as well as gene sets. Samples for Body Atlas data are obtained
371 from publicly available studies that are internally curated, annotated, and processed. Body Atlas
372 measurements are generated from all available RNA expression studies that used Affymetrix U133 Plus or
373 U133A Genechip Arrays for human studies. The results from 128 human tissue samples were incorporated
374 from 1,067 arrays; 157 human cell types from 1,474 arrays; and 359 human cancer cell lines from 376 arrays.
375 Gene queries return a list of relevant tissues or cell types rank-ordered by absolute gene expression and
376 grouped by body systems or across all body systems. In the current analysis, we determined the
377 expression levels of the apolipoproteins ApoA1, ApoA2, ApoB, ApoC1, ApoC2, ApoC3, ApoD,
378 ApoE, ApoH, ApoL1, ApoL2 and ApoO in liver tissue. We used an analysis protocol developed by
379 NextBio, the details of which have been described previously (20).
380 **cDNA microarray.** Expression profiling was generated using the 4 x 44 K whole human genome
381 oligo-microarray ver.2.0 G4845A (Agilent Technologies) as previously described (54). Raw data
382 were imported into Subio platform ver.1.12 (Subio) for database management and quality control.
383 Raw intensity data were normalized against GAP-DH expression levels for further analysis. These
384 raw data have been accepted by GEO (a public repository for microarray data, aimed at storing
385 MIAME). Access to data concerning this study may be found under GEO experiment accession
386 number GSE32886.
387 **Cell lines.** All cell lines were cultured at 37°C under the conditions of a humidified atmosphere and
388 5% CO_2. The human hepatocellular carcinoma-derived Huh7 and human embryonic kidney-derived
389 293T cells were obtained from Japanese Collection of Research Bioresources (JCRB) Cell Bank
390 (JCRB0403 and JCRB9068), and maintained in DMEM (Sigma) supplemented with 100 U/ml
391 penicillin, 100 μg/ml streptomycin, and 10% fetal calf serum (FCS). The Huh7-derived cell line
392 Huh7.5.1 was kindly provided by F. Chisari. Huh7 cells harboring JFH1-based HCV-SGR were
393 prepared according to the method of a previous report (54) and maintained in DMEM containing
394 10% FCS and 1mg/ml G418 (Nakalai Tesque).
395 **Plasmids.** The cDNA clones of pri-miR-122, ApoA1, ApoA2, ApoC1, ApoC2, ApoC3, ApoE,
396 ApoH, and AcGFP were inserted between the XhoI and XbaI sites of lentiviral vector
397 pCSII-EF-RfA, which was kindly provided by M. Hijikata, and the resulting plasmids were
398 designated pCSII-EF-miR-122, pCSII-EF-MT-apolipoproteins, and pCSII-EF-AcGFP, respectively.
399 The deletion mutants of ApoC1 and ApoE were amplified by PCR and introduced into pCSII-EF.
400 pHH-JFH1-E2p7NS2mt contains three adaptive mutations in pHH-JFH1 (55). The pFL-J6/JFH1
401 plasmid that encodes the entire viral genome of the chimeric strain of HCV-2a, J6/JFH1, was kindly
402 provided by Charles M. Rice (8). pTH/JFH1 (genotype 1b) and pS310/JFH1 (genotype 3a) were
403 used for the production of chimeric viruses (22, 23). The plasmid pX330, which encodes hCas9 and
404 sgRNA, was obtained from Addgene (Addgene plasmid 42230). The fragments of guided RNA
405 targeting the MTTP gene were inserted into the Bbs1 site of pX330 and designated pX330-MTTP.
406 The plasmids used in this study were confirmed by sequencing with an ABI 3130 genetic analyzer
407 (Life Technologies).
408 **Antibodies.** Mouse monoclonal antibodies to HCV core, β-actin and Calnexin were purchased from
409 Thermo Scientific and Sigma Aldrich, respectively. Mouse anti-ApoA1, ApoB, ApoC1, ApoE and
410 ApoH antibodies were purchased from Cell Signaling, ALerCHEK Inc., Abnova, NOVUS
411 Biologicals, and Santa Cruz Biotechnology, respectively. Rat anti-ApoA2 and Sheep anti-ApoC2
412 antibodies were purchased from R&D systems. Rabbit anti-NS5A antibody was prepared as

413 described previously (54). Alexa Fluor (AF) 488-conjugated anti-rabbit or mouse IgG antibodies,
414 and AF594-conjugated anti-mouse IgG2a antibodies were purchased from Life Technologies.
415 **Gene silencing.** A small interfering RNA (siRNA) pool targeting various apolipoproteins
416 (siGENOME SMARTpool) and control nontargeting siRNA were purchased from Dharmacon, and
417 transfected into cells using Lipofectamine RNAi MAX (Life Technologies) according to the
418 manufacturer's protocol. A human shRNA library was purchased from Takara Bio Inc.
419 **Preparation of viruses.** Upon transfection of pHH-JFH1-E2p7NS2mt or *in vitro* transcribed
420 TH/JFH1, J6/JFH1 and S310/JFH1 RNA into Huh7.5.1 cells, HCV in the supernatant was collected
421 after serial passages, and infectious titers were determined by a focus-forming assay and expressed in
422 focus-forming units (FFU) (22, 23, 54). To compare the localization of core protein, J6/JFH1 was
423 used in Figure 6E. Pseudoparticles expressing HCV envelope glycoprotein were generated in 293T
424 cells as previously reported (5), and infectivity was assessed by luciferase expression using the
425 Bright-Glo™ Luciferase assay system (Promega) and expressed in relative light units (RLU).
426 **Lipofection and lentiviral gene transduction.** The lentiviral vectors and ViraPower Lentiviral
427 Packaging Mix (Life Technologies) were co-transfected into 293T cells by Trans IT LT-1 (Mirus),
428 and the supernatants were recovered at 48 h post-transfection. The lentivirus titer was determined by
429 the Lenti-XTM qRT-PCR Titration Kit (Clontech), and the expression levels and AcGFP were
430 determined at 48 h post-inoculation.
431 **Immunoblotting.** Cells lysed on ice in lysis buffer (20 mM Tris-HCl [pH7.4], 135 mM NaCl, 1%
432 Triton-X 100, 10% glycerol) supplemented with a protease inhibitor mix (Nacalai Tesque) were
433 boiled in loading buffer and subjected to 5-20% gradient SDS-PAGE. The proteins were transferred
434 to polyvinylidene difluoride membranes (Millipore) and reacted with the appropriate antibodies. The
435 immune complexes were visualized with SuperSignal West Femto Substrate (Pierce) and detected
436 by the LAS-3000 image analyzer system (Fujifilm).
437 **Generation of gene-knockout Huh7 cell lines.** Custom ZFN plasmids were designed to bind and
438 cleave the ApoB, ApoE and MTTP genes and were obtained from Sigma Aldrich. Huh7 cells were
439 transfected with *in vitro* transcribed ZFNs mRNA or pX330-MTTP by Lipofectamine 2000 (Life
440 Technologies), and single cell clones were established by the single cell isolation technique. To
441 screen for gene-knockout Huh7 cell clones, mutations in target loci were determined by using a
442 Surveyor assay as previously described (56). Frameshift of the genes and deficiencies of protein
443 expression were confirmed by direct sequencing and immunoblotting analysis, respectively.
444 **Enzyme-linked immunosorbent assay (ELISA).** Protein concentrations of ApoB or ApoE in the
445 culture supernatants were determined by using ELISA immunoassay kits (Alercheck Inc.) according
446 to the manufacturer's protocol.
447 **Quantitative RT-PCR.** Total RNA was extracted from cells by using an RNeasy minikit (Qiagen)
448 and the first-strand cDNA synthesis and qRT-PCR were performed with TaqMan EZ RT-PCR core
449 reagents and a ViiA7 system (Life Technologies), respectively, according to the manufacturer's
450 protocol. The primers for TaqMan PCR targeted to the noncoding region of HCV RNA were
451 synthesized as previously reported (54). Taqman® Gene expression assays were used as the primers
452 and probes targeting to apolipoproteins (Life Technologies). Fluorescent signals were analyzed with
453 the ViiA7 system.
454 **Immunofluorescence assay.** Cells cultured on glass slides were fixed with 4% paraformaldehyde
455 (PFA) in phosphate buffered saline (PBS) at room temperature for 30 min, permeabilized for 20 min
456 at room temperature with PBS containing 0.2% Triton after being washed three times with PBS, and
457 blocked with PBS containing 2% FCS for 1 h at room temperature. The cells were incubated with
458 PBS containing the appropriate primary antibodies at room temperature for 1 h, washed three times
459 with PBS, and incubated with PBS containing AF488- or AF594-conjugated secondary antibodies at
460 room temperature for 1 h. For lipid-droplet staining, cells incubated in medium containing 20 μg/ml
461 BODIPY® for 20 min at 37°C were washed with pre-warmed fresh medium and incubated for 20
462 min at 37°C. Cell nuclei were stained with DAPI. Cells were observed with a FluoView FV1000

laser scanning confocal microscope (Olympus).

***In vitro* transcription, RNA transfection, and colony formation.** The plasmid pSGR-JFH1 was linearized with XbaI, and treated with mung bean exonuclease. The linearized DNA was transcribed *in vitro* by using the MEGAscript T7 kit (Life Technologies) according to the manufacturer's protocol. The *in vitro* transcribed RNA (10 μg) was electroporated into Huh7 cells at 10^7 cells/0.4 ml under conditions of 190 V and 975 μF using a Gene Pulser™ (Bio-Rad) and plated on DMEM containing 10% FCS. The medium was replaced with fresh DMEM containing 10% FCS and 1 mg/ml G418 at 24 h post-transfection. The remaining colonies were cloned by using a cloning ring (Asahi Glass) or fixed with 4% PFA and stained with crystal violet at 4 weeks post-electroporation.

Intracellular infectivity. Intracellular viral titers were determined according to a method previously reported (10). Briefly, cells were extensively washed with PBS, scraped, and centrifuged for 5 min at 1000 × *g*. Cell pellets were resuspended in 500 μl of DMEM containing 10% FCS and subjected to three cycles of freezing and thawing using liquid nitrogen and a thermo block set to 37 °C. Cell lysates were centrifuged at 10,000 × *g* for 10 min at 4 °C to remove cell debris. Cell-associated infectivity was determined by a focus-forming assay.

Electron microscopy and correlative FM-EM analysis. Correlative fluorescence microscopy-electron microscopy (FM-EM) allows individual cells to be examined both in an overview with fluorescence microscopy and in a detailed subcellular-structure view with electron microscopy. Cells infected with HCVcc were examined by the correlative FM-EM method as described previously (57).

Buoyant density fractionation. Culture supernatants of cells infected with HCVcc were concentrated 50 times by using Spin-X UF concentrators (Corning), and the intracellular proteins collected after freeze-and-thaw were applied to the top of a linear gradient formed from 10-40% OptiPrep (Axis-Shield) in PBS and spun at 32,000 rpm for 16 h at 4 °C by using an SW41 Ti rotor (Beckman Coulter). Aliquots of 10 consecutive fractions were collected, and the infectious titer and density were determined.

Proteinase K digestion protection assay. The proteinase K digestion protection assay was performed as described previously (37). Briefly, cells were extensively washed with PBS, scraped, and centrifuged for 5 min at 1000 × *g*. The cell pellets were resuspended in 500 μl of PBS and subjected to three cycles of freezing and thawing using liquid nitrogen and a thermo block set to 37 °C. The cell lysates were centrifuged at 10,000 × *g* for 10 min at 4 °C to remove cell debris. The cell lysates were then incubated with 50 μg/ml proteinase K (Life Technologies) in the presence or absence of 5% Triton-X for 1 h on ice, and the digestion was terminated by addition of PMSF (Wako Chemical Industries).

Statistics. The data for statistical analyses are the average of three independent experiments. Results were expressed as the means ± standard deviation. The significance of differences in the means was determined by Student's *t*-test.

Acknowledgements

We thank M. Tomiyama for her secretarial work and M. Ishibashi and Y. Sugiyama for their technical assistance. We also thank M. Hijikata, T. Wakita, R. Bartenschlager, F. Chisari, and M. Whitt for providing experimental materials.

References

1. Maasoumy B, Wedemeyer H (2012) Natural history of acute and chronic hepatitis C. Best. Pract. Res. Clin. 26: 410-412.
2. Jacobson IM, McHutchison JG, Dusheiko G, Di Bisceglie AM, Reddy KR, et al. (2011) Telaprevir for previously untreated chronic hepatitis C virus infection. N. Engl. J. Med. 364: 2405-2416.
3. Sulkowski MS, Gardiner DF, Rodriguez-Torres M, Reddy KR, Hassanein T, et al. (2014)

513 Daclatasvir plus Sofosbuvir for previously treated or untreated chronic HCV infection. N. Engl.
514 J. Med. 370: 211-221.
515 4. Janssen HL, Reesink HW, Lawitz EJ, Zeuzem S, Rodriguez-Torres M, et al. (2013) Treatment
516 of HCV infection by targeting microRNA. N. Engl. J. Med. 368: 1685-1694.
517 5. Bartosch B, Dubuisson J, Cosset F (2003) Infectious hepatitis C virus pseudo-particles
518 containing functional E1-E2 envelope protein complexes. J. Exp. Med. 197: 633-642.
519 6. Lohmann V, Korner F, Koch JO, Herian U, Theilmann L, et al. (1999) Replication of
520 subgenomic hepatitis C virus RNAs in a hepatoma cell line. Science. 285: 110-113.
521 7. Wakita T, Pietschmann T, Kato T, Date T, Miyamoto M, et al. (2005) Production of infectious
522 hepatitis C virus in tissue culture from a cloned viral genome. Nat. Med. 11: 791-796.
523 8. Lindenbach BD, Evans MJ, Syder AJ, Wolk B, Tellinghuisen TL, et al. (2005) Complete
524 replication of hepatitis C virus in cell culture. Science. 309: 623-626.
525 9. Jirasko V, Montserret R, Lee JY, Gouttenoire J, Moradpour D, et al. (2010) Structural and
526 functional studies of nonstructural protein 2 of the hepatitis C virus reveal its key role as
527 organizer of virion assembly. PLoS Pathog. 6: e1001233.
528 10. Gastaminza P, Cheng G, Wieland S, Zhong J, Liao W, et al. (2008) Cellular determinants of
529 hepatitis C virus assembly, maturation, degradation, and secretion. J. Virol. 82: 2120-2129.
530 11. Jiang J, Luo G (2009) Apolipoprotein E but not B is required for the formation of infectious
531 hepatitis C virus particles. J. Virol. 83: 12680-12691.
532 12. Andre P, Komurian-Pradel F, Deforges S, Perret M, Berland L, et al. (2002) Characterization of
533 Low- and Very-Low-Density hepatitis C virus RNA-containing particles. J. Virol. 76:
534 6919-6928.
535 13. Saito H, Lund-Katz S, Phillips MC. (2004) Contribution of domain structure and lipid
536 interaction to the functionality of exchangeable human apolipoproteins. Prog. Lipid Res. 43:
537 350-380.
538 14. Narayanaswami V, Kiss RS, Weers PM. (2010) The helix bundle: A reversible lipid binding
539 motif. Comp. Biochem. Physiol. A Mol. Integr. Physiol. 155: 123-133.
540 15. Mancone C, Steindler C, Santangelo L, Simonte G, Vlassi C, et al. (2011) Hepatitis C virus
541 production requires apolipoprotein A-1 and affects its association with nascent low-density
542 lipoproteins. Gut. 60: 378-386.
543 16. Da Costa D, Turek M, Felmee DJ, Girardi E, Pfeffer S, et al. (2012) Reconstitution of the entire
544 hepatitis C virus life cycle in nonhepatic cells. J. Virol. 86: 11919-11925.
545 17. Porteus MH, Carroll D (2005) Gene targeting using zinc finger nucleases. Nat. Biotechnol. 23:
546 967-973.
547 18. Zhang F, Cong L, Lodato S, Kosuri S, Church GM, et al. (2011) Efficient construction of
548 sequence-specific TAL effectors for modulating mammalian transcription. Nat. Biotechnol. 29:
549 149-153.
550 19. Mali P, Yang L, Esvelt KM, Aach J, Guell M, et al. (2013) RNA-guided human genome
551 engineering via Cas9. Science. 339: 823-826.
552 20. Kupershmidt I, Su QJ, Grewal A, Sundaresh S, Halperin I, et al. (2010) Ontology-based
553 meta-analysis of global collections of high-throughput public data. PLoS One. 5: e13066.
554 21. Hussain MM, Shi J, Dreizen P (2003) Microsomal triglyceride transfer protein and its role in
555 apoB-lipoprotein assembly. J. Lipid Res. 44: 22-32.
556 22. Takebe Y, Saucedo CJ, Lund G, Uenishi R, Hase S, et al. (2013) Antiviral lectins from Red and
557 Blue-Green Algae show potent *in vitro* and *in vivo* activity against hepatitis C virus. PLoS One.
558 8: e64449.
559 23. Kim S, Date T, Yokokawa H, Kono T, Aizaki H, et al. (2014) Development of hepatitis C virus
560 genotype 3a cell culture system. Hepatology. doi: 10.1002/hep.27197.
561 24. Miyanari Y, Atsuzawa K, Usuda N, Watashi K, Hishiki T, et al. (2007) The lipid droplet is an
562 important organelle for hepatitis C virus production. Nat. Cell Biol. 9: 961-969.